J Fluoresc (2008) 18:1007–1019
DOI 10.1007/s10895-008-0388-0

ORIGINAL PAPER

Photophysical and Complexation Properties of Benzenesulfonamide Derivatives with Different Donor and Acceptor Moieties

G. Özturk · M. Förstel · Y. Ergun · S. Alp · W. Rettig

Received: 14 February 2008 / Accepted: 16 May 2008 / Published online: 17 June 2008

Abstract Pyrrolobenzosulfonamide, indolobenzosulfonamide and carbazolobenzosulfonamide derivatives with different acceptor groups were synthesized and their photophysical properties were compared. The electron donor linking sites are found to influence the emission characteristics of these compounds while acceptor linking sites have no noticeable effects on the spectral properties. P2-A5 which is a C–C linked pyrrole derivative exhibited different spectral properties from the C–N linked pyrrole derivatives. The complexation properties of the molecules were also investigated employing Na (I), Ca (II), Li (I), Mg (II), Zn (II) and Cu (II) ions.

Keywords Fluorescence · Sulfonamide · Photophysics · Pyrrole · Indole · Carbazole

Introduction

Organic compounds substituted both by an electron donor and an electron acceptor groups are of major interest in chemistry and have thus been subjected to intensive experimental and theoretical investigations [1–8]. This interest originates from various possible applications: Donor–acceptor substituted aromatic systems have high non-linear optical properties which is an important prerequisite for their application for data storage, holographic material, optical switches, or molecular wires [4, 5]. The molecules are also of commercial interest as laser dyes and fluorescence probes due to their sensitive response to changes in their microenvironment [6, 7].

The design and synthesis of molecular systems capable of signaling various guest molecules or ions are of current interest in host–guest chemistry [1, 7, 8]. Among the numerous analytical methods that are available for the detection of cations, those based on fluorescent sensors offer several distinct advantages in terms of sensitivity, selectivity, response time and local observations.

Twisted Intramolecular Charge-Transfer (TICT) has been investigated very thoroughly [9, 10], and many types of fluorescent probes have been developed which are possibly connected to TICT [1, 7, 11–13]. Most of them are derived from *N,N*-dimethylaminobenzonitrile (DMABN) [12] which shows an intrinsically very small fluorescence quantum yield. Moreover, the complexation mostly occurred on the donor moiety, as for many other often used dyes [14, 15] which leads to disappearance or weakening of the CT band on complexation, and to blue shifts of the absorption and fluorescence, which are more difficult to use analytically.

Some of the TICT compounds, however, show sizeable fluorescence quantum yields, especially those DMABN derivative where the DMA group has been replaced by a benzenic aromatic donor system, i.e. a benzo-linked heterocycle like indole or carbazole [11]. These compounds also show strong solvatochromic redshifts indicating their high dipole moment and CT character. Recent work has shown, that an analytical advantage is gained if the complexation leads to a redshift of the fluorescence. In terms of TICT compounds, this has been shown to occur with the amide derivatives of DMABN [12] as well as with some donor–acceptor biphenyl [7], if complexation occurs not on the donor moiety, as usual, but on the acceptor moiety. For the DMABN-amides [12], this is readily

G. Özturk · Y. Ergun · S. Alp
Department of Chemistry, Faculty of Arts and Sciences,
University of Dokuz Eylul,
35160 Tinaztepe, Izmir, Turkey

M. Förstel · W. Rettig (✉)
Institut für Chemie, Humboldt-Universität zu Berlin,
Brook-Taylor-Str. 2,
12489 Berlin, Germany
e-mail: rettig@chemie.hu-berlin.de

possible, if the complexing aza-crown ether is part of the amide function. Unfortunately, in case of the amides, an nπ*-channel quenches the fluorescence [12] so that the fluorescence quantum yields of these compounds are very small. When a sulfonamide group is used as an acceptor, quenching via the nπ*-channel is less important [16–22].

In this work we synthesized new TICT-derivatives with benzo-linked heterocyclic with different acceptor groups of *N,N*-diethyl (A5), *N,N*-bis(2-methoxyethyl) (A9) and 1,4,7,10-tetraoxa-13-azacyclopentadecane-13-yl (A15C5) and donor groups of pyrrole (P), indole (I) and carbazole (C). The idea is to create an acceptor complexation site leading to emission redshifts from a CT state which has the potential of larger sensitivity to a given metal ion—and which therefore may be able to lead to increased ion selectivity.

In the first part of our studies, we investigated the influence of the donor and acceptor group on spectral and photophysical properties of the derivatives. In the second part the interactions of the derivatives with Na (I), Ca (II), Li (I), Mg (II), Zn (II) and Cu (II) ions were investigated in acetonitrile and the observed changes in spectral properties were compared.

Experimental

Solvents and reagents

All the chemicals used for the synthesis of the fluorescent probes were purchased from Merck and Fluka. The metal ion perchlorates obtained from ALFA and Aldrich were of the highest purity commercially available and were dried in a vacuum dessicator over P_2O_5. All the solvents employed for spectroscopy were of Merck Uvasol quality and directly used without further purification.

Synthesis

The compounds investigated and their abbreviations are summarized in Scheme 1.

N,N-diethyl-4-iodobenzenesulfonamide (B-A5) [23] Diethylamine (0.4 mL, 3.8 mmol) was dissolved in pyridine (10 mL). The resulting solution was cooled to 0 °C and 4-iodobenzenesulfonylchloride (1 g, 3.3 mmol) was added. The reaction mixture was stirred for 12 h at room temperature. Then water was added (15 mL) and the resulting mixture was extracted with 3×30 mL of chloroform. The residue was then chromatographed on silica gel using chloroform as eluent. After the evaporation of the solvent the solid was recrystallysed from chloroform/ethanol mixture and pure A was obtained. Yield: 1.16 g. ^{1}H-NMR (300 MHz, $CDCl_3$), δ (ppm): 1.28–1.09 (t, J=7.1 Hz, 6H, –CH_3), 3.24–3.18 (q, J=7.1 Hz, 4H, –CH_2), 7.51–7.49 (d, J=8.6 Hz, 2H, PhH), 7.84–7.82 (d, J=8.5 Hz, 2H, PhH).

N,N-bis(2-methoxyethyl)-4-iodobenzenesulfonamide (B-A9) B-A9 was prepared according to the same procedure as for B-A5, using bis(2-methoxyethyl)amine (0.6 mL, 4.1 mmol), 4-iodobenzenesulfonylchloride (1 g, 3.3 mmol) and pyridine (10 mL). Yield: 1.08 g. ^{1}H-NMR (300 MHz, $CDCl_3$), δ (ppm): 3.26 (s, 6H, –CH_3), 3.39–3.36 (t, J=5.7 Hz, 4H, N–CH_2), 3.50–3.47 (t, J=5.9 Hz, 4H, O–CH_2), 7.54–7.51 (d, J=8.6 Hz, 2H, PhH), 7.84–7.81 (d, J=8.6 Hz, 2H, PhH).

1,4,7,10-tetraoxa-13-azacyclopentadecane-13-yl-4-iodobenzenesulfonamide (B-A15C5) B-A15C5 was prepared according to the same procedure as for B-A5, using 1-aza-15-crown-5 (1 g, 4.6 mmol), 4-iodobenzenesulfonylchloride (1.4 g, 4.7 mmol) and pyridine (10 mL). Yield: 0.975 g. ^{1}H-NMR (300 MHz, $CDCl_3$), δ (ppm): 3.29–3.26 (t, J=6.3 Hz, 4H, N–CH_2–CH_2), 3.64–3.59 (m, 14H, OCH_2-crown), 3.74–3.71 (t, J=6.3 Hz, 4H, N–CH_2–CH_2), 7.52–7.49 (d, J=8.6 Hz, 2H, PhH), 7.84–7.82 (d, J=8.7 Hz, 2H, PhH).

N,N-diethyl-4-(1H-pyrrol-2-yl)benzenesulfonamide (P2-A5) [24] After degassing of a mixture of *N,N*-diethyl-4-iodobenzenesulfonamide (0.500 g, 1.5 mmol), pyrrole (0.1 mL, 1.4 mmol), NaOAc (0.121 g, 1.5 mmol) and *N*-methyl-2-pyrrolidon (10 mL), the additive triphenylphosphine (7.03 mg, 2 mol%) and the catalyst [$Pd(OAc)_2$] (3.01 mg, 1 mol%) were added and the mixture was heated to 140 °C for 96 h under nitrogen. The reaction was conducted under vigorous stirring and then the reaction mixture was cooled to room temperature. The reaction mixture was then diluted with 100 mL of water and the resulting mixture was extracted with 3×20 mL of ethyl acetate. The combined organic layers were washed three times with 15 mL H_2O and dried over Na_2SO_4 and the solvent was evaporated. The residue was then chromatographed on silica gel using a 95:5 mixture of chloroform and ethanol. After the evaporation of the solvent the solid was recrystallysed from ethyl acetate/hexane mixture and pure A-a1 was obtained. Yield: 0.120 g. ^{1}H-NMR (300 MHz, $CDCl_3$), δ (ppm): 1.13–1.09 (t, J=7.1 Hz, 6H, –CH_3), 3.26–3.20 (q, J=7.3 Hz, 4H, –CH_2), 6.32–6.30 (m, 1H, pyrrole–H), 6.64–6.62 (m, 1H, pyrrole–H), 6.93–6.91 (m, 1H, pyrrole–H), 7.54–7.52 (d, J=8.5 Hz, 2H, PhH), 7.77–7.74 (d, J=8.5 Hz, 2H, PhH), 8.58 (s, 1H, NH). ^{13}C-NMR (75 MHz, $CDCl_3$), δ (ppm): 14.2 (2C, –CH_3), 42.3 (2C, –CH_2), 108.2 (1C, pyrrole–C), 110.7 (1C, pyrrole–C), 120.8 (1C, pyrrole–C), 123.7 (2C, PhC), 127.6 (2C, PhC), 130.3 (1C, pyrrole–C), 136.5 (1C, PhC), 136.8 (1C, PhC).

N,N-diethyl-4-(1H-pyrrol-1-yl)benzenesulfonamide (P-A5) [25] After degassing of a mixture of *N,N*-diethyl-4-iodobenzenesulfonamide (0.500 g, 1.5 mmol), pyrrole (0.1 mL,

Scheme 1 Compounds investigated and their abbreviations

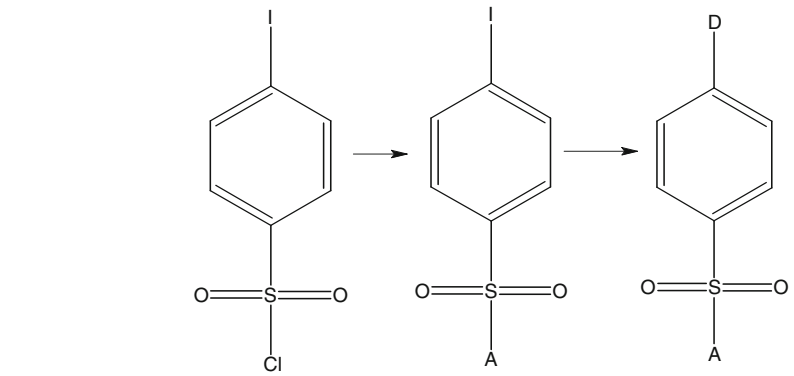

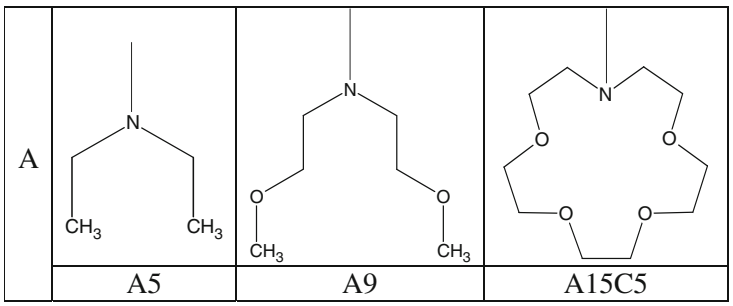

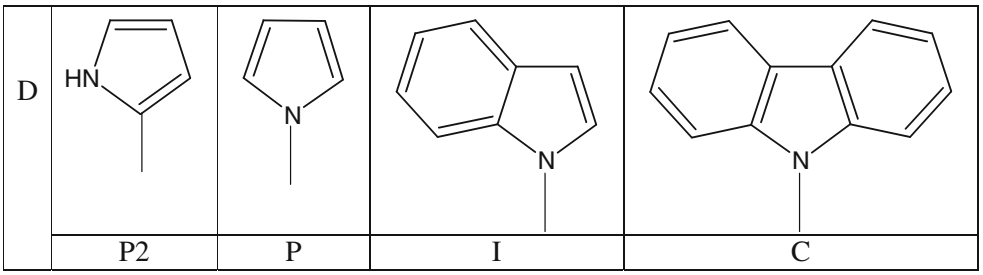

Compound	A	D
P2-A5	A5	P2
P-A5	A5	P
P-A9	A9	P
P-A15C5	A15C5	P
I-A5	A5	I
I-A9	A9	I
I-A15C5	A15C5	I
C-A9	A9	C

1.4 mmol), Cs_2CO_3 (0.586 g, 1.8 mmol) and toluene (20 mL), the additive diphenylphosphinoferrocene (15.0 mg, 1.5 mol%) and the catalyst [$Pd(OAc)_2$] (4.0 mg, 1 mol%) were added and the mixture was heated to 120 °C for 72 h under nitrogen. The reaction was conducted under vigorous stirring and then the reaction mixture was cooled to room temperature. The reaction mixture was then diluted with 100 mL of water and the resulting mixture was extracted with 3×20 mL of ethyl acetate. The combined organic layers were washed three times with 15 mL H_2O and dried over Na_2SO_4 and the solvent was evaporated. The crude solid the starting materials and (by)products were chromatographed on silica gel using 1:1 mixture of petroleum ether and dichloromethane as eluent. After the evaporation of the solvent the residue was chromatographed on silica gel with a 2:1 mixture of hexane and ethyl acetate. After evaporation of the solvent the solid was recrystallysed from ethyl acetate/hexane mixture and pure A-a2 was obtained. Yield: 0.072 g. ^{1}H-NMR (300 MHz, $CDCl_3$), δ (ppm): 1.15–1.11 (t, J=7.2 Hz, 6H, –CH_3), 3.27–3.22 (q, J=7.2 Hz, 4H, –CH_2), 6.38–6.37 (t, J=2.1 Hz, 2H, pyrrole–H), 7.13–7.12 (t, J=2.1 Hz, 2H, pyrrole–H), 7.48–7.46 (d, J=8.8 Hz, 2H, PhH),

7.85–7.83 (d, J=8.75 Hz, 2H, PhH). ^{13}C-NMR (75 MHz, $CDCl_3$), δ (ppm): 14.2 (2C, –CH_3), 42.0 (2C, –CH_2), 111.8 (2C, pyrrole–C), 119.0 (2C, pyrrole–C), 119.9 (2C, PhC), 128.8 (2C, PhC), 136.9 (1C, PhC), 143.4 (1C, PhC).

N,N-bis(2-methoxyethyl)-4-(1H-pyrrol-1-yl)benzenesulfonamide (P-A9) P-A9 was prepared according to the same procedure as for P-A5, using *N,N*-bis(2-methoxyethyl)-4-iodobenzenesulfonamide (0.500 g, 1.3 mmol), pyrrole (0.1 mL, 1.4 mmol), Cs_2CO_3 (0.526 g, 1.6 mmol), the additive diphenylphosphinoferrocene (13.4 mg, 1.5 mol%) and the catalyst [$Pd(OAc)_2$] (3.6 mg, 1 mol%) in toluene (20 mL). Yield: 0.045 g. ^{1}H-NMR (300 MHz, $CDCl_3$), δ (ppm): 3.27 (s, 6H, –CH_3), 3.42–3.39 (t, J=5.7 Hz, 4H, N–CH_2), 3.53–3.50 (t, J=5.9 Hz, 4H, O–CH_2), 6.37–6.36 (t, J= 2.2 Hz, 2H, pyrrole–H), 7.13–7.12 (t, J=2.3 Hz, 2H, pyrrole–H), 7.48–7.46 (d, J=8.8 Hz, 2H, PhH), 7.87–7.85 (d, J= 8.7 Hz, 2H, PhH). ^{13}C-NMR (75 MHz, $CDCl_3$), δ (ppm): 48.5 (2C, –CH_3), 58.8 (2C, O–CH_2), 71.4 (2C, N–CH_2), 111.8 (2C, pyrrole–C), 119.0 (2C, pyrrole–C), 119.7 (2C, PhC), 129.0 (2C, PhC), 136.5 (1C, PhC), 143.6 (1C, PhC).

1,4,7,10-tetraoxa-13-azacyclopentadecane-13-yl-4-(1H-pyrrol-1-yl)benzenesulfonamide (P-A15C5) P-A15C5 was prepared according to the same procedure as for P-A5, using 1,4,7,10-tetraoxa-13-azacyclopentadecane-13-yl-4-iodobenzenesulfonamide (0.500 g, 1.1 mmol), pyrrole (0.1 mL, 1.4 mmol), Cs_2CO_3 (0.407 g, 1.25 mmol), the additive diphenylphosphinoferrocene (10.4 mg, 1.5 mol%) and the catalyst [$Pd(OAc)_2$] (2.8 mg, 1 mol%) in toluene (20 mL). The crude product was chromatographed on silica gel using 2:1 mixture of hexane and ethyl acetate and then with 1:2 mixture of hexane and ethyl acetate. Yield: 0.039 g. ^{1}H-NMR (300 MHz, $CDCl_3$), δ (ppm): 3.32–3.29 (t, J=6.3 Hz, 4H, N–CH_2–CH_2), 3.63–3.60 (m, 14H, OCH_2-crown), 3.76–3.73 (t, J=6.3 Hz, 4H, N–CH_2–CH_2), 6.37–6.36 (t, J=2.3 Hz, 2H, pyrrole–H), 7.12–7.11 (t, J= 2.2 Hz, 2H, pyrrole–H), 7.48–7.45 (d, J=8.8 Hz, 2H, PhH), 7.85–7.83 (d, J=8.9 Hz, 2H, PhH). ^{13}C-NMR (75 MHz, $CDCl_3$), δ (ppm): 50.7 (2C, crown), 70.2 (2C, crown), 70.3 (2C, crown), 70.7(2C, crown), 71.0 (2C, crown), 111.9 (2C, pyrrole–C), 119.0 (2C, pyrrole–C), 119.9 (2C, PhC), 129.0 (2C, PhC), 135.5 (1C, PhC), 143.7 (1C, PhC).

N,N-diethyl-4-(1H-indol-1-yl)benzenesulfonamide (I-A5) I-A5 was prepared according to the same procedure as for P-A5, using *N,N*-diethyl-4-iodobenzenesulfonamide (0.500 g, 1.5 mmol), indole (0.176 g, 1.5 mmol), Cs_2CO_3 (0.586 g,

Table 1 Spectral and photophysical data of pyrrole derivatives

Probe	Solvent	λ_{abs}[a] (nm)	λ_{flu}[b,c] (nm)	$\Delta\lambda$[d] (nm)	φ_f[e]	τ_f[f] (ns)	k_f[g] (10^7 s^{-1})	k_{nr}[h] (10^7 s^{-1})
P-A5	Hex	278	314	36	0.0018	1.02	0.18	97.86
	BOB	278	355	77	0.0073			
	EOE	278	383	105	0.0202			
	THF	279	411	132	0.0332			
	ACN	277	443	166	0.0482	9.00	0.54	10.56
P-A9	Hex	277	317	40	0.0060	1.06	0.57	93.77
	BOB	278	358	80	0.0214			
	EOE	278	390	112	0.0269			
	THF	278	416	138	0.0487			
	ACN	277	452	175	0.0507	9.70	0.52	9.79
P-A15C5	Hex	277	341	64	0.0031	*<2.47>	0.13	40.36
	BOB	277	357		0.0296			
	EOE	277	382	105	0.0320			
	THF	278	415	137	0.0572			
	ACN	277	451	174	0.0618	9.32	0.66	10.09
P2-A5	Hex	312	347	35	0.0123	*<0.56>	2.20	176.36
	BOB	322	360	38	0.0728			
	EOE	322	364	42	0.4590			
	THF	321	372	60	0.5073			
	ACN	318	381	63	0.5320	1.74	30.57	26.90

[a] Absorption maxima
[b] Emission maxima
[c] Excitation wavelength was fixed at the absorption maximum
[d] Stokes shift, i.e., the wavelength difference between the longest wavelength absorption band (or shoulder) and the emission maximum
[e] Fluorescence quantum yield
[f] Fluorescence lifetime: $*<\tau>=\left(A_1\tau_1^2+A_2\tau_2^2\right)/\left(A_1\tau_1+A_2\tau_2\right)$
[g] Radiative rate constant, $k_f=\varphi_f/\tau_f$
[h] Non-radiative rate constant, $k_{nr}=(1-\varphi_f)/\tau_f$

Table 2 Spectral and photophysical data of indole and carbazole derivatives

Probe	Solvent	λ^1_{abs} [a] (nm)	λ^2_{abs} [a] (nm)	λ_{flu} [b,c] (nm)	$\Delta\nu$ [d] (cm^{-1})	φ_f [e]	τ_f [f] (ns)	k_f [g] (10^7 s^{-1})	k_{nr} [h] (10^7 s^{-1})
I-A5	Hex	268	308	333	2,437	0.0216	*<0.81>	2.67	120.79
	BOB	268	309	357	4,351	0.0869			
	EOE	268	309	375	5,696	0.1195			
	THF	268	311	394	6,774	0.1543			
	ACN	268	308	429	9,157	0.1168	7.29	1.60	12.12
I-A9	Hex	268	309	337	2,689	0.0307	*<0.63>	4.87	153.86
	BOB	268	310	360	4,481	0.1109			
	EOE	268	309	381	6,116	0.1271			
	THF	268	311	401	7,217	0.1740			
	ACN	268	308	438	9,636	0.1139	7.03	1.62	12.60
I-A15C5	Hex	267	309	335	2,512	0.0386	*<0.67>	5.76	143.49
	BOB	267	310	358	4,326	0.1128			
	EOE	268	309	376	5,767	0.1278			
	THF	269	310	397	7,174	0.1761			
	ACN	268	309	435	9,374	0.1170	7.55	1.55	11.70
C-A9	Hex	292	313	342	2,709	0.1971	1.94	10.16	41.39
	BOB	292	313	357	3,937	0.3069			
	EOE	291	313	375	5,282	0.3640			
	THF	292	313	390	6,307	0.4939			
	ACN	291	311	423	8,514	0.3065	7.95	3.86	8.72

[a] Absorption maxima
[b] Emission maxima
[c] Excitation wavelength was fixed at the absorption maximum
[d] Stokes shift, i.e., the wavelength difference between the longest wavelength absorption band (or shoulder) and the emission maximum
[e] Fluorescence quantum yield
[f] Fluorescence lifetime: $*<\tau>=\left(A_1\tau_1^2+A_2\tau_2^2\right)/(A_1\tau_1+A_2\tau_2)$
[g] Radiative rate constant, $k_f=\varphi_f/\tau_f$
[h] Non-radiative rate constant, $k_{nr}=(1-\varphi_f)/\tau_f$

1.8 mmol), the additive diphenylphosphinoferrocene (15.0 mg, 1.5 mol%) and the catalyst [$Pd(OAc)_2$] (4.0 mg, 1 mol%) in toluene (20 mL). Yield: 0.010 g. ^{1}H-NMR (300 MHz, $CDCl_3$), δ (ppm): 1.19–1.15 (t, J=7.2 Hz, 6H, –CH_3), 3.32–3.27 (q, J=7.1 Hz, 4H, –CH_2), 6.73–6.72 (d, J= 4.3 Hz, 1H, indole–H), 7.27–7.17 (m, 2H, indole–H), 7.35–7.34 (d, J=3.6 Hz, 1H, indole–H), 7.69–7.59 (m, 2H, indole–H), 7.64–7.61 (d, J=11.0 Hz, 2H, PhH), 7.95–7.93 (d, J= 9.0 Hz, 2H, PhH). ^{13}C-NMR (75 MHz, $CDCl_3$), δ (ppm): 14.3 (2C, –CH_3), 42.2 (2C, –CH_2), 105.3 (1C, indole–C), 110.4 (1C, indole–C), 121.2 (1C, indole–C), 121.5 (1C, indole–C), 123.0 (1C, indole–C), 123.8 (2C, PhC), 127.3 (1C, indole–C), 128.7 (2C, PhC), 130.1 (1C, indole–C), 135.4 (1C, indole–C), 137.7 (1C, PhC), 143.2 (1C, PhC).

N,N-bis(2-methoxyethyl)-4-(1H-indol-1-yl)benzenesulfonamide (I-A9) B-b was prepared according to the same procedure as for P-A5, using *N,N*-bis(2-methoxyethyl)-4-iodobenzenesulfonamide (0.500 g, 1.3 mmol), indole (0.158 g, 1.3 mmol), Cs_2CO_3 (0.526 g, 1.6 mmol), the additive diphenylphosphinoferrocene (13.4 mg, 1.5 mol%) and the catalyst [$Pd(OAc)_2$] (3.6 mg, 1 mol%) in toluene (20 mL). Yield: 0.280 g. ^{1}H-NMR (300 MHz, $CDCl_3$), δ (ppm): 3.34 (s, 6H, –CH_3), 3.52–3.48 (t, J=5.6 Hz, 4H, N–CH_2), 3.62–3.58 (t, J=5.6 Hz, 4H, O–CH_2), 6.77–6.76 (d, J=3.4 Hz, 1H, indole–H), 7.32–7.21 (m, 2H, indole–H), 7.38–7.37 (d, J=3.8 Hz, 1H, indole–H), 7.73–7.63 (m, 2H, indole–H), 7.68–7.65 (d, J=8.7 Hz, 2H, PhH), 8.03–8.00 (d, J=8.3 Hz, 2H, PhH). ^{13}C-NMR (75 MHz, $CDCl_3$), δ

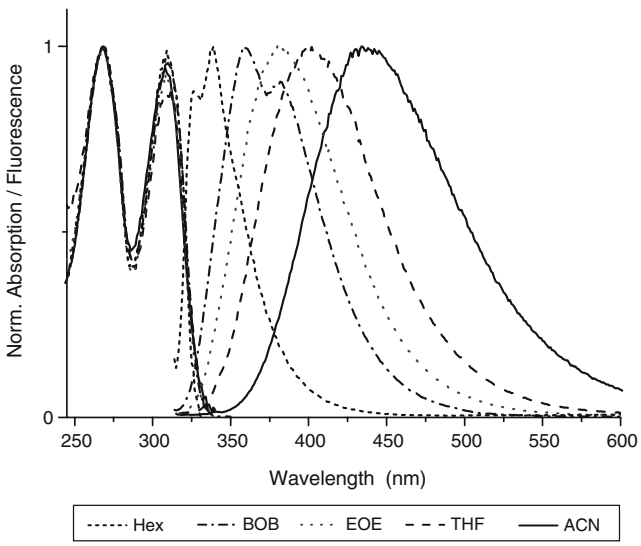

Fig. 1 Normalised absorption and fluorescence spectra of I-C9 for variation of solvent polarity

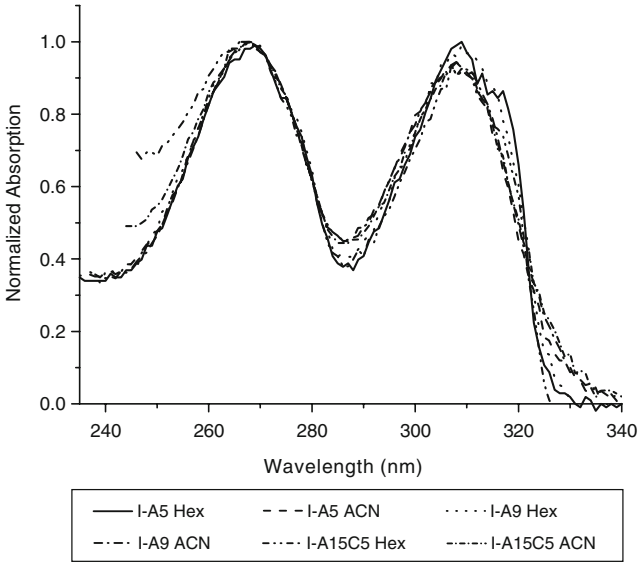

Fig. 2 Normalized absorption spectra of I-A5, I-A9 and I-A15C5 in Hex and ACN for variation of the acceptor group with constant donor (indole) moiety

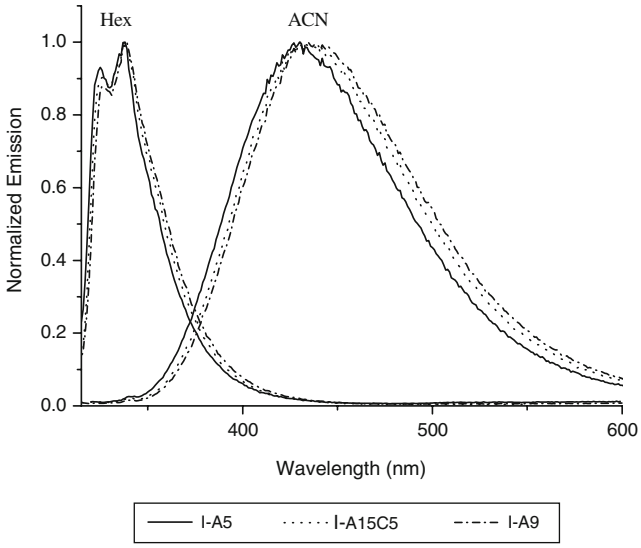

Fig. 3 Normalized fluorescence spectra of I-A5, I-A9 and I-A15C5 in Hex and ACN for variation of the acceptor group for equal donor (indole) moiety

(ppm): 48.6 (2C, $–CH_3$), 58.8 (2C, $O–CH_2$), 71.5 (2C, $N–CH_2$), 105.3 (1C, indole–C), 110.4 (1C, indole–C), 121.2 (1C, indole–C), 121.5 (1C, indole–C), 123.1 (1C, indole–C), 123.7 (2C, PhC), 127.3 (1C, indole–C), 129.0 (2C, PhC), 130.0 (1C, indole–C), 135.4 (1C, indole–C), 137.3 (1C, PhC), 143.3 (1C, PhC).

1,4,7,10-tetraoxa-13-azacyclopentadecan-13-yl-4-(1H-indol-1-yl)benzenesulfonamide (I-A15C5) C-b was prepared according to the same procedure as for P-A5, using 1,4,7,10-tetraoxa-13-azacyclopentadecane-13-yl-4-iodobenzenesulfonamide (0.500 g, 1.1 mmol), indole (0.121 g, 1.1 mmol), Cs_2CO_3 (0.407 g, 1.25 mmol), the additive diphenylphosphinoferrocene (10.4 mg, 1.5 mol%) and the catalyst [$Pd(OAc)_2$] (2.8 mg, 1 mol%) in toluene (20 mL). The crude product was chromatographed on silica gel using 2:1 mixture of hexane and ethyl acetate and then with 1:2 mixture of hexane and ethyl acetate. Yield: 0.049 g. ^{1}H-NMR (300 MHz, $CDCl_3$), δ (ppm): 3.38–3.35 (t, J=6.3 Hz, 4H, $N–CH_2–CH_2$), 3.66–3.61 (m, 14H, OCH_2-crown), 3.80–3.77 (t, J=6.3 Hz, 4H, $N–CH_2–CH_2$), 6.73–6.72 (d, J=3.3 Hz, 1H, indole–H), 7.28–7.17 (m, 2H, indole–H), 7.34–7.33 (d, J=3.5 Hz, 1H, indole–H), 7.69–7.59 (m, 2H, indole–H), 7.64–7.62 (d, J=8.8 Hz, 2H, PhH), 7.96–7.94 (d, J=8.8 Hz, 2H, PhH). ^{13}C-NMR (75 MHz, $CDCl_3$), δ (ppm): 50.8 (2C, crown), 70.3 (2C, crown), 70.4 (2C, crown), 70.7(2C, crown), 71.0 (2C, crown), 105.3 (1C, indole–C), 110.4 (1C, indole–C), 121.2 (1C, indole–C), 121.5 (1C, indole–C), 123.1 (1C, indole–C), 123.7 (2C, PhC), 127.3 (1C, indole–C), 128.9 (2C, PhC), 129.7 (1C, indole–C), 135.1 (1C, indole–C), 136.3 (1C, PhC), 144.9 (1C, PhC).

N,N-bis(2-methoxyethyl)-4-(9H-carbazol-9-yl)benzenesulfonamide (C-A9) B-c was prepared according to the same procedure as for P-A5, using *N,N*-bis(2-methoxyethyl)-4-iodobenzenesulfonamide (0.500 g, 1.3 mmol), carbazole (0.225 g, 1.3 mmol), Cs_2CO_3 (0.526 g, 1.6 mmol), the additive diphenylphosphinoferrocene (13.4 mg, 1.5 mol%) and the catalyst [$Pd(OAc)_2$] (3.6 mg, 1 mol%) in toluene (20 mL). Yield: 0.145 g. ^{1}H-NMR (300 MHz, $CDCl_3$), δ (ppm): 3.32 (s, 6H, $–CH_3$), 3.52–3.49 (t, J=5.9 Hz, 4H, $N–CH_2$), 3.60–3.57 (t, J=5.8 Hz, 4H, $O–CH_2$), 7.33–7.29 (m, 2H, carbazole–H), 7.45–7.40 (m, 4H, carbazole–H), 7.74–7.71 (d, J=8.8 Hz, 2H, PhH), 8.08–8.05 (d, J=8.8 Hz, 2H,

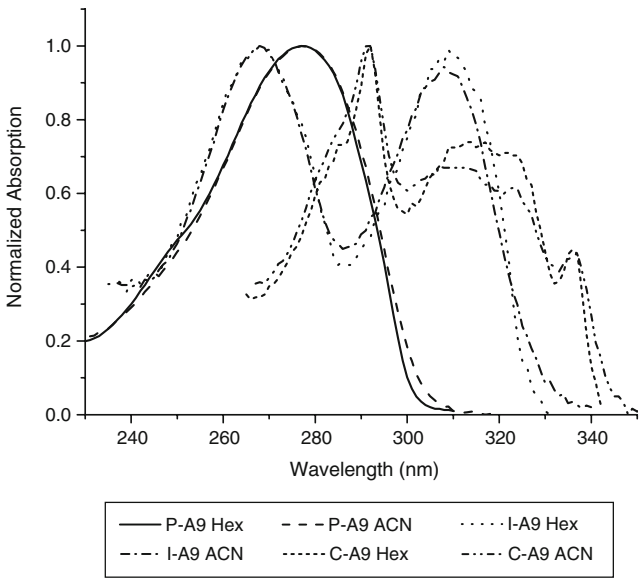

Fig. 4 Normalized absorption spectra of P-A9 (pyrrole), I-A9 (indole) and C-A9 (carbazole) in Hex and ACN for variation of the donor with constant acceptor group ($SO_2–N(CH_2CH_3)_2$)

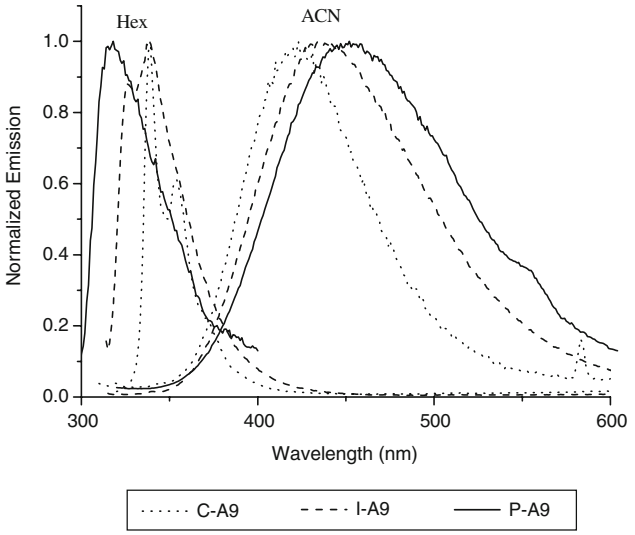

Fig. 5 Normalised fluorescence spectra of P-A9 (pyrrole), I-A9 (indole) and C-A9 (carbazole) in Hex and ACN for variation of the donor with constant acceptor group (SO_2–$N(CH_2CH_3)_2$)

PhH), 8.14–8.12 (d, J=7.7 Hz, 2H, carbazole–H). ^{13}C-NMR (75 MHz, $CDCl_3$), δ (ppm): 48.7 (2C, –CH_3), 58.9 (2C, O–CH_2), 71.5 (2C, N–CH_2), 109.6 (2C, carbazole), 120.6 (2C, carbazole), 120.8 (2C, carbazole), 123.9 (2C, PhC), 126.3 (2C, carbazole), 126.9 (2C, carbazole), 129.1 (2C, PhC), 138.5 (1C, PhC), 140.1 (2C, carbazole), 141.6 (1C, PhC).

Apparatus

The chemical structures of the synthesized compounds were confirmed by ^{1}H and ^{13}C NMR. ^{1}H and ^{13}C NMR spectra were recorded on a Bruker Avauce 300 NMR spectrometer at 400 and 75 MHz respectively.

Steady state spectra

Absorption spectra were measured on an ATI UNICAM Series UV–Vis Spectrometer UV4-021113 and fluorescence spectra on an SLM AMINCO-Bowmann series 2 Luminescence Spectrofluorimeter fitted with a 150 W Xenon lamp. All fluorescence spectra were corrected for detector response.

Fluorescence quantum yields

Fluorescence quantum yields were determined relative to quinine bisulphate in 0.1 N H_2SO_4 and calculated on the basis of Eq. 1 [26].

$$\Phi_f = \Phi_f^0\left(n^2A^0\int I_f(\lambda_f)d\lambda_f \Big/ n_0^2A\int I_f^0(\lambda_f)d\lambda_f\right) \quad (1)$$

where n_0 and n are the refractive indices of the solvent, A^0 and A (0.095–0.105) are the absorbances, Φ_f^0(= 52%) [27] and Φ_f are the quantum yields, and the integrals denote the (computed) area of the corrected fluorescence bands, each parameter being for the standard (index 0) and the sample solution, respectively. The relative experimental error of the quantum yields is around ±10%.

The relative quantum yield values were calculated according to the Eq. 2

$$\Phi_{rel} = \left(\int I(\lambda)_{ML}OD_L\right)/\left(\int I(\lambda)_L OD_{ML}\right) \quad (2)$$

where $\int I(\lambda)_{ML}$ and $\int I(\lambda)_L$ are the computed area of the corrected fluorescence bands of the ligand with the complexed metal cation and of the uncomplexed ligand, respectively. OD_L and OD_{ML} denote the optical densities of ligand and the ligand interacted with metal cation, respectively.

Fluorescence lifetime

Fluorescence decay measurements were performed using the principle of time correlated single photon counting (TC-SPC) [28] with a setup using a passively mode-locked Ti: sapphire laser from SpectraPhysics pumped by a Millenia pro diode-pumped, CW visible laser system. Pulse duration is appr. 80 fs and pulse frequency is appr. 81 MHz. The excitation wavelength was obtained by third harmonic

Table 3 Decay times, τ_i, and their amplitudes in Hex

Probe	τ_1[a]	A_1[b]	τ_2[a]	A_2[b]	$<\tau>$[c]	φ_1[d] (rel)	φ_2[d] (rel)
P2-A5	0.688	0.0084878	0.109	0.0150560	0.56	0.78	0.22
P-A5	1.018		–				
P-A9	1.056		–				
P-A15C5	2.61	0.0021387	0.31	0.0009589	2.47	0.72	0.28
I-A5	1.52	0.0021116	0.14	0.0244456	0.81	0.48	0.52
I-A9	1.01	0.0041069	0.18	0.0190420	0.63	0.26	0.74
I-A15C5	0.28	0.0200180	1.51	0.0017141	0.67	0.68	0.32
C-A9	1.94		–				

[a] Decay time
[b] Amplitude
[c] $<\tau>=\left(A_1\tau_1^2+A_2\tau_2^2\right)/(A_1\tau_1+A_2\tau_2)$ [d] $\phi_1(\text{rel})=A_1\tau_1^2/(A_1\tau_1+A_2\tau_2);\phi_2(\text{rel})=A_2\tau_2^2/(A_1\tau_1+A_2\tau_2)$

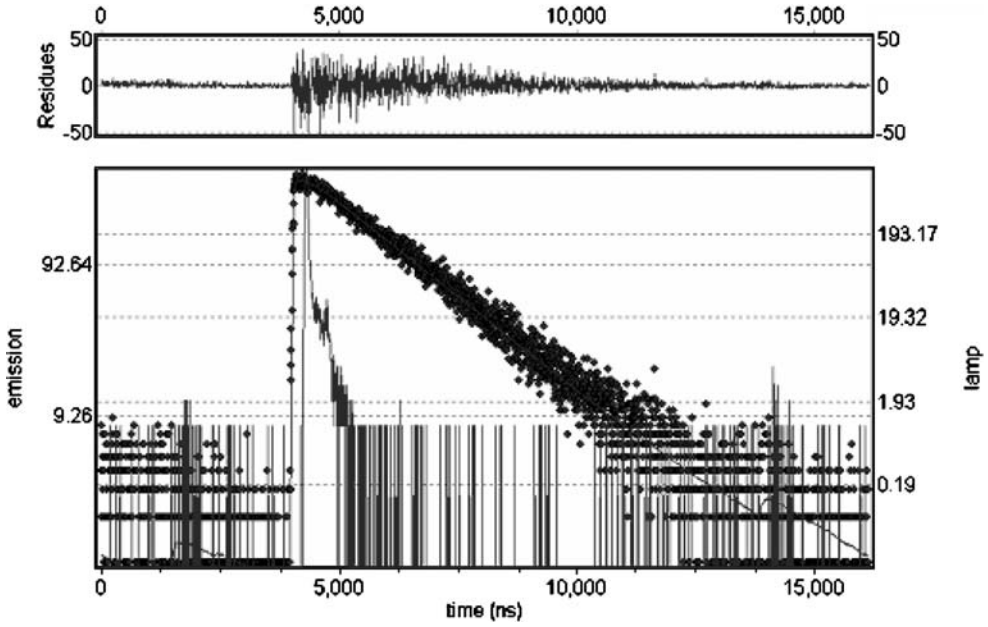

Fig. 6 Fluorescence decay of P2-A5 in ACN. Excitation at 259 nm, observation at 381 nm

generation from the fundamental wavelength of 800 nm. Fluorescence and scatter were detected by a microchannel plate photomultiplier (MCP, Hamamatsu R 1564 U-01 operated at −30 °C) coupled by quartz fiberoptics to the emission monochromator (Oriel MS257). The signal from a constant fraction discriminator (CFD, Tennelec 454) was used as the start pulse for the time to amplitude converter (TAC, Tennelec TC864) operating in reverse mode. Stop pulses were obtained by imaging a small part of the excitation light with a photodiode (HAS-X-S-1G4-SI, FEMTO® Messtechnik GmbH). The MCP pulses were amplified using a Hamamatsu C4890 wide band amplifier. The count rate was held below 6 k counts per second to avoid pile-up effects. A multichannel analyzer (Fast Comtec MCDLAP) was used for data accumulation. The instrument response function was detected using a stray solution at the excitation wavelength and had a width of 50–70 ps.

Results and discussion

Spectral and photophysical data

The absorption and emission data of pyrrolobenzosulfonamide (P-A), indolobenzosulfonamide (I-A) and carbazolobenzosulfonamide (C-A) derivatives are compared in Tables 1 and 2. The absorption spectra of the P derivatives are a single band, whereas the absorption spectra of I and C are double bands (Figs. 1, 2 and 4). The absorption bands of each compound are independent of solvent polarity and do not show any noticeable shifts in their maximum in

Table 4 Dipole moments for the ground and excited states

Probe	a^a (Å)	$\upsilon_f/\Delta f'^b$ (cm^{-1})	valign="top">μ_g^c (D)	μ_e^d (D)	a^e (Å)	μ_e^f (D)
P2-A5	5.7	8,892	5.56	13.8	5.7	13.8
P-A5	5.7	33,298	4.55	22.9	5.7	22.9
P-A9	6.0	33,818	4.55	25.4	5.7	23.1
P-A15C5	7.2	33,024*	4.55	31.1	5.7	22.9
I-A5	7.4	23,888	4.66	28.3	7.4	28.3
I-A9	8.0	24,577	4.66	31.7	7.4	28.5
I-A15C5	8.6	24,222	4.66	34.9	7.4	28.4
C-A9	8.4	18,774	5.31	30.2	8.4	30.2

[a] Onsager radius derived from the mass density formula considering the whole molecule including the alkane chains and the crown moiety
[b] Solvatochromic slope: *for P-A15C5 the highly structured hexane spectrum indicates that the character is mostly LE in contrast to the other compounds. This spectrum was therefore omitted.
[c] Ground state dipole moment
[d] Excited state dipole moment using the Onsager radius according to footnote a
[e] Onsager radius derived from the length of the chromophore system alone
[f] Excited state dipole moment using the Onsager radius according to footnote e

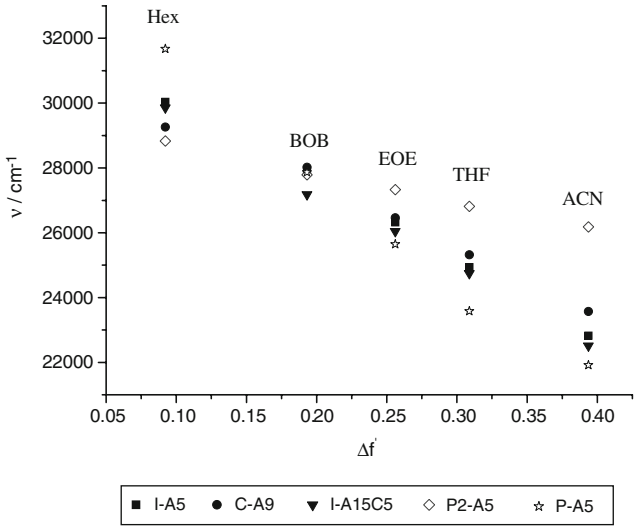

Fig. 7 Solvatochromic fluorescence plots

solvents of increasing polarity (Fig. 1). However, the fluorescence spectra show a significant solvatochromic effect, indicating a charge transfer (CT) character of the emitting state (Fig. 1). The fluorescence maximum exhibits a red-shift with increasing the solvent polarity for all compounds investigated. The emission maxima of pyrrolobenzosulfonamide derivatives are red shifted in acetonitrile in comparison to N–phenylpyrrole (PB) [29]. Likewise, the emission maxima of indolesulfonamide derivatives are red shifted in acetonitrile in comparison to phenylcarbazole (PC) previously reported in the literature [30].

The absorption and emission spectra of derivatives with the same donor group, but different acceptor groups are almost identical, indicating no influence of the acceptor group on spectral properties (Figs. 2 and 3). This is as expected, because the acceptor property is nearly the same in all derivatives. The results given in Tables 1 and 2, Figs. 4 and 5 indicate that the donor group has a strong influence on the absorption and emission properties. In case of indole and carbazole derivatives in comparison to C–N linked pyrrole derivatives in all the solvents, the absorption maximum is red shifted, but the emission maximum is blue shifted in THF, EOE and ACN and red shifted in Hex (Table 3).

By changing the linking sites in the pyrrole–bezosulfonamide pair (P and P2) interesting spectral changes are observed (Table 1). Similar effects have been observed for pyrrolobenzonitriles reported previously in the literature [31]. While the absorption maximum of P2-A5, which is a C–C linked pyrrolobenzosulfonamide derivative, is in the range of 312–318 nm in the solvents of different polarity, the absorption maximum of the C–N linked pyrrole derivatives is in the range of 277–279 nm, i.e. highly blue shifted. However, the emission maximum of C–N linked pyrrole derivatives is red shifted in the range of medium polar to highly polar solvents in comparison to P2-A5 derivative, but blue shifted in Hex. The red-shift in emission with increasing the solvent polarity is much smaller for P2-A5 derivative than for P-A5 derivative indicating a smaller change in the dipole moment of P2-A5 from the ground state to the excited state. In the non-polar hexane, the absorption maximum of P2-A5 is, however, significantly red-shifted with respect to P-A5 indicating a larger mesomeric interaction in the ground state.

The solvent-induced shifts for all derivatives except for P2-A5 are very large in polar solvents indicating a considerable energetic stabilization of the excited state in polar solvents. Moreover, the similar Stokes shift values for the derivatives with the same donor group indicate that a similar stabilization occurs in these compounds irrespective of the size of the acceptor groups which varies significantly. This suggests that the size of the cavity which has to be

Table 5 Spectroscopic properties of the complexes of P-A15C5 with metal ions in acetonitrile at room temperature

Compound	λ_{abs}[a] (nm)	ε[b] (L mol cm^{-1})	λ_{em}[c] nm (cm^{-1})	$\Delta\lambda_{St}$[d] (nm)	$\Delta\lambda_{cp-fp}$[e] (nm)	FWHM[f] (cm^{-1})	Φ_{rel}[g]
P-A15C5	277	20,400	451 (22,203)	174		6,159	
–Ca^{2+}	283	16,600	458 (22,058)	175	7	7,472	0.1481
–Na^{+}	280	19,000	480 (20,936)	200	29	6,634	0.5733
–Li	279	17,800	485 (20,704)	206	34	6,936	0.4603
–Mg^{2+}	279	16,500	457 (21,794)	178	6	6,732	0.5553
–Zn^{2+}	279	130,000	452 (22,894)	173	2	8,539	0.0908
–Cu^{2+}	281	98,000	450 (22,234)	169	−1	9,619	0.0035

[a] Absorption maximum
[b] Molar extinction coefficient
[c] Emission maximum
[d] Stokes shift, i.e., the wavelength difference between the longest wavelength absorption band (or shoulder) and the emission maximum
[e] Spectral shift in emission between free probe and complexed probe with "fp" and "cp" equaling free probe and complexed probe
[f] Half width of the emission band
[g] Relative quantum yield, see Eq. 2
Metal ion to ligand concentration ratios were M:L=10,000:1. The ligand concentration is 1×10^{-5} M.

Table 6 Spectroscopic properties of the complexes of I-A15C5 with metal ions in acetonitrile at room temperature

Compound	λ_{abs}[a] (nm)	ε[b] (L mol cm^{-1})	λ_{em}[c] nm (cm^{-1})	$\Delta\lambda$[d] (nm)	$\Delta\lambda_{cp-fp}$[e] (nm)	FWHM[f] (cm^{-1})	Φ_{rel}[g]
I-A15C5	309	13,400	435 (22,922)	126		5,528	
–Ca^{2+}	312	12,700	447 (22,357)	135	12	6,072	0.1442
–Na^{+}	312	13,300	460 (21,774)	148	25	5,897	0.3649
–Li^{+}	312	12,300	465 (21,569)	153	30	6000	0.2958
–Mg^{2+}	309	12,700	440 (22,577)	131	5	5,788	0.4818
–Zn^{2+}	309	120,400	440 (22,931)	131	5	6,763	0.0253
–Cu^{2+}	309	83,600	433 (23,177)	124	–2	6,145	0.0057

[a] Lowest energy absorption band
[b] Molar extinction coefficient
[c] Emission maximum
[d] Spectral shift, i.e., the wavelength difference between the longest wavelength absorption band (or shoulder) and the emission maximum
[e] Spectral shift in emission between free probe and complexed probe with "cp" and "fp" equaling free probe and complexed probe
[f] Half width of the emission peak
[g] Relative quantum yield, see Eq. 2
Metal ion to ligand concentration ratios were M:L=10,000:1. The ligand concentration is 1×10^{-5} M.

used in the solvatochromic equations (Eqs. 3–5 below) is not determined by the compound itself but more by the extension of the chromophore π-system.

The fluorescence quantum yield values show only a small variation in the range of medium polar to highly polar solvents for all the compounds investigated. However, the quantum yield values in the non-polar solvent hex are significantly lower. The quantum yield values of indole and carbazole derivatives are higher than the values of pyrrole derivatives. P2-A showed the highest quantum yield values among all the compounds investigated. All the pyrrole derivatives examined in this study have higher quantum yield values than the *N*-pyrrolo-4-benzonitrile derivatives reported previously in the literature [32]. Indolobenzosulfonamide derivatives exhibit higher quantum yield values in comparison to phenylcarbazole (PC) in acetonitrile [29].

The lifetime values in Hex are much shorter than in ACN for all benzosulfonamide derivatives investigated, except for P2-A5 for which the lifetime in acetonitrile is also short (Fig. 6, Tables 1 and 2). Using the φ_f and τ_f values, the radiative (k_f) and nonradiative (k_{nr}) rates could be compared. It can be seen that for the N-substituted P derivative, k_f is very small, both in hex and in ACN, suggesting a forbidden emissive state probably of TICT nature. P2-A5, however, shows allowed fluorescence from a normal intramolecular CT state. For the indole derivative, the radiative rate is significantly smaller in ACN than in hex which can also be due to an emissive average conformation closer to perpendicularity in the more polar solvent, consistent with the TICT model. The short lifetimes in Hex are due to the strongly enhanced k_{nr} in this solvent.

The solvatochromic slopes were analysed to get quantitative information on the dipole moments for all compounds, by applying the Mataga equation (Eq. 3) [33, 34] and the resulting values are collected in Table 4. The plot of emission maximum vs. the polarity parameter $\Delta f'$ is shown in Fig. 7.

The excited-state dipole moments μ_e are calculated from a plot of the solvatochromic shift of the emission maxima vs. solvent polarity (Fig. 7), and are calculated using the Mataga equation (Eq. 3), where μ_e and μ_g are the ground and excited-state dipole moments, respectively, h is the Planck's constant, $\in_0$ the permittivity constant of vacuum and c is the velocity of light. υ_f are the emission maxima and $\Delta f'$ is the solvent polarity parameter, consisting of the dielectric constant ε and the refractive index n. The Onsager radii a were calculated from the mass-density formula (Eq. 4) by assuming equal densities ρ, and the ground-state dipole moments, μ_e, are calculated by using the AM1 semi empirical method embedded in the AMPAC

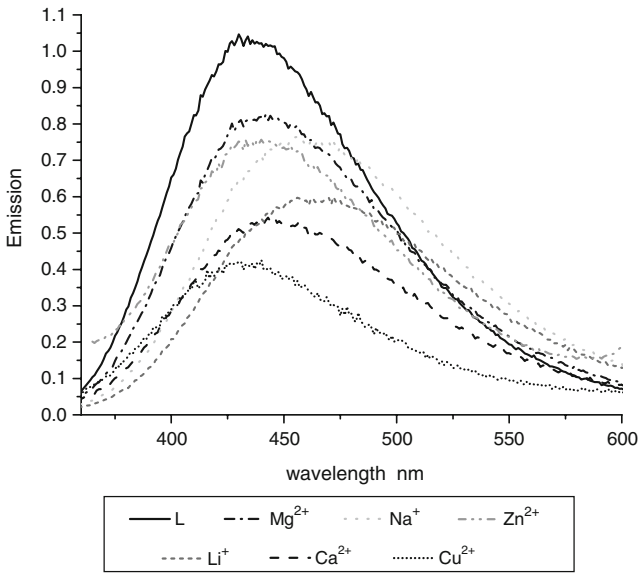

Fig. 8 Changes in emission spectra for I-A15C5 in ACN for 1:10,000 ligand (L) to metal (M) ion concentration. The probe concentration was 10^{-5} M. The intensities are increased arbitrarily for good visibility and the relative quantum yield values are given in Table 6

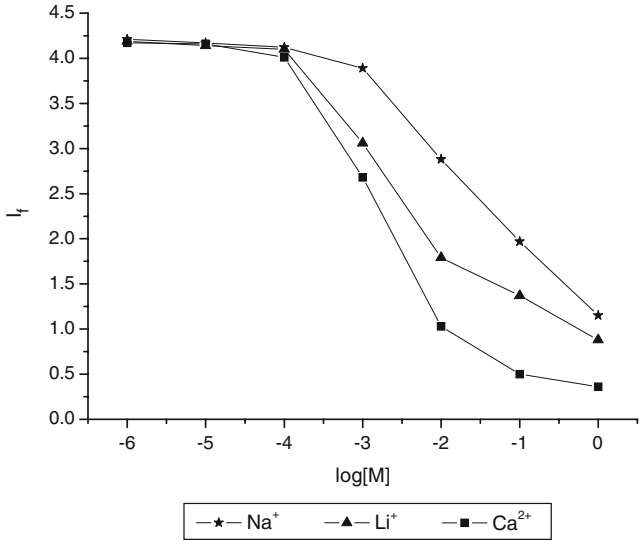

Fig. 9 Complexation-induced changes in emission for P-A15C5 derivative in ACN after exposure to Na^+, Li^+ and Ca^{2+}. The probe concentration was 10^{-5} M

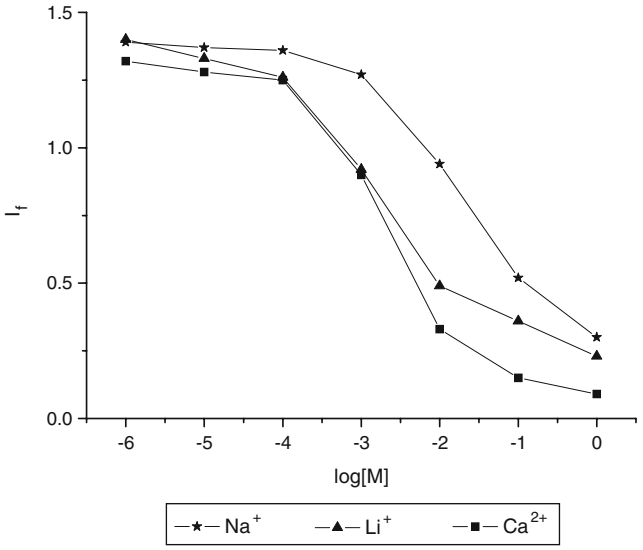

Fig. 11 Complexation-induced changes in emission for I-A15C5 derivative in acetonitrile after exposure to Na^+, Li^+ and Ca^{2+}. The probe concentration was 10^{-5} M

software package (AMPAC 6.0 and AMPAC 6.55. Semichem, Inc., Shawnee, USA, 1997).

$$\upsilon_f = -\left(2\Delta f'/4\pi \in_0 hca^3\right)\mu_e\left(\mu_e - \mu_g\right) + \text{const.} \quad (3)$$

$$\text{With } \Delta f' = (\varepsilon - 1)/(2\varepsilon + 1) - {}^1\!/_2\left(n^2 - 1\right)\Big/\left(2n^2 + 1\right) \quad (4)$$

$$a = \left(3M/4\pi N_A \rho\right)^{1/3} \quad (5)$$

The high dipole moment values in the excited state indicate that the excited state is of CT nature in these compounds.

It is shown in Table 4, that the excited state dipole moment μ_e and the ground to excited state change in dipole moment $\Delta\mu$ of P2-A5 are both smaller than that of P-A derivatives. These results can be rationalized by assuming that the CT states of these compounds have different nature, as suggested by the k_f results, see above. A TICT state with a strongly twisted conformation is expected to have a larger μ_e than a Mesomeric Intramolecular Charge-Transfer (MICT) state [35] with an emissive average conformation closer to planarity and corresponds to a larger change in dipole moment $\Delta\mu$ from the ground to excited state as observed for P-A5 and P2-A5.

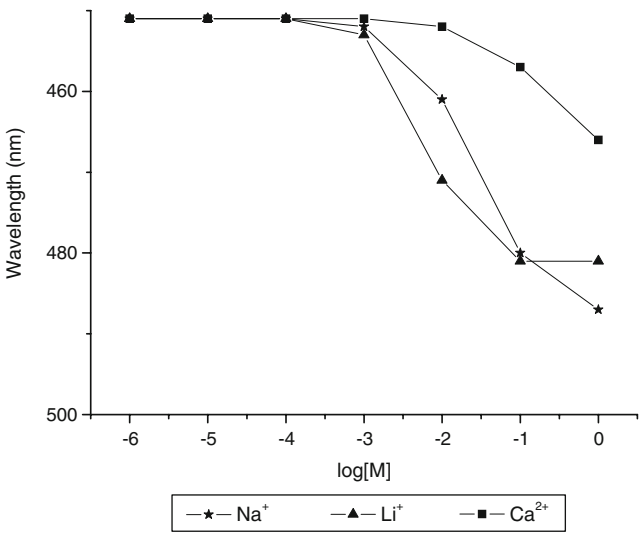

Fig. 10 Complexation induced shifts in wavelength for P-A15C5 derivative in acetonitrile after exposure to Na^+, Li^+ and Ca^{2+}. The probe concentration was 10^{-5} M

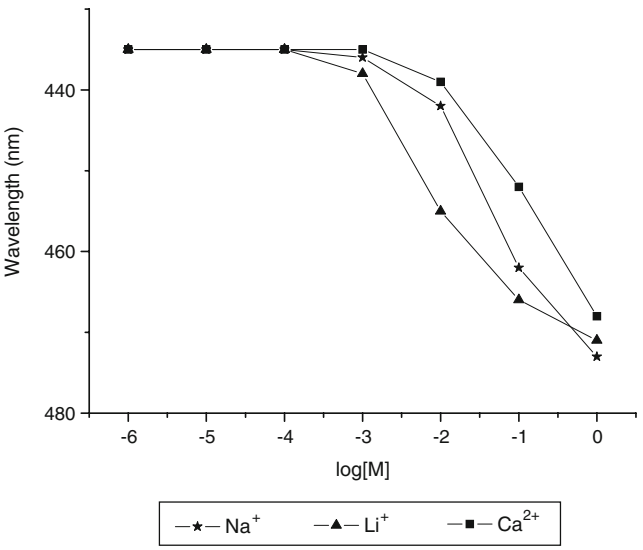

Fig. 12 Complexation induced shifts in wavelength for I-A15C5 derivative in ACN after exposure to Na^+, Li^+ and Ca^{2+}. The probe concentration was 10^{-5} M

Interestingly, all solvatochromic slopes within each "family" are equal with experimental error, see the A5, A9 and A15C5 derivatives of the P and A series. Similar CT dipole moment values only result if the Onsager radius is derived by omitting the alkane chains on the acceptor. There is no reason why these CT dipole moments should be different. We therefore conclude that in long elongated chromophores with nonconjugated chains, these do not contribute to the effective Onsager radius.

Complexation studies

To conceive the potential of the derivatives as fluorescent reporters for metal ions, the spectroscopic properties of their interaction with Na (I), Ca (II), Li (I), Mg (II), Zn (II) and Cu (II) ions were investigated in acetonitrile. The spectroscopic properties of the cation complexes of P-A15C5 and I-A15C5 which consist of monoaza-15-crown-5 acceptor group summarized in Tables 5 and 6, indicate red shifts in emission as expected for an increase of the acceptor strength due to ion complexation (Fig. 8). Among all metal ions employed the highest red shift values were observed for Na (I), Ca (II) and Li (I) ions. Thus, P-A15C5 and I-A15C5 derivatives were titrated with Na (I), Ca (II) and Li (I). Upon addition of Na (I), Ca (II) and Li (I) metal salts to 10^{-5} M solutions of P-A15C5 and I-A15C5 in acetonitrile, the corresponding changes observed in fluorescence intensity and emission wavelength are given in Figs. 9–12. As follows from the titrations shown in Figs. 9–12, the responses to metal cations for P-A15C5 and I-A15C5 are similar. The highest red shift value is obtained for Li^+ ions for both derivatives investigated (Tables 5 and 6, Figs. 10 and 12).

In order to investigate the effect of acceptor group on the complexation properties of the molecules, I-A5 with an *N, N*-diethyl group and I-A9 with an *N,N*-bis(2-methoxyethyl) group in the acceptor part were also investigated with Na (I), Ca (II), Li (I), Mg (II), Zn (II) and Cu (II) ions in acetonitrile and no changes in absorption and emission wavelength were detected, but only a decrease in emission intensity was observed, indicating no complexation, but only quenching effects.

No attempts were made to determine the corresponding complexation constants as large metal ion to ligand concentration ratios were required for complete acceptor complexation. Complete complexation at large concentration ratios was verified by further increasing the ion concentration without spectral effect.

Conclusion

It is shown that the absorption and emission spectra of derivatives with the same donor group, but different yet related acceptor groups are almost identical. However the donor group has a strong influence on absorption and emission properties. Absorption and emission data reveal that the excited state CT character of P-A5 and P2-A5 is different. The MICT character (large mesomeric interaction for near-planar geometries) of P2-A5 as compared to the TICT character of P-A derivatives is supported by its reduced excited-state dipole moment and the enhanced radiative rate constant value. The spectroscopic properties of the cation complexes of P-A15C5 and I-A15C5 which contain the monoaza-15-crown-5 acceptor group exhibit red shifts in emission as compared to the uncomplexed compounds. Among the metal cations investigated the strongest shifts of the emission wavelength were observed for Na (I), Ca (II) and Li (I) ions.

Acknowledgments The Scientific and Technological Research Council of Turkey's 2214-Reseach Fellowship Program is gratefully acknowledged. We thank to Dr. Julia Bricks, Dr. Wilfried Weigel, Mrs. Annette Rothe and Lars Lasoggaa for experimental help.

References

1. Malval, Lapouyade R, Leger, Jarry C (2003) Tripodal ligand incorporating dual fluorescent ionophore: a coordinative control of photoinduced electron transfer. Photochem Photobiol Sci 2:259–266
2. Parusel ABJ (2000) A DFT/MRCI study on the excited state charge transfer states of *N*-pyrrolobenzene, *N*-pyrrolobenzonitrile and 4-*N,N*-dimethylaminobenzonitrile. Phys Chem Chem Phys 2:5545–5552
3. Shao H, Chen X, Wang Z, Lu P (2007) Synthesis and fluorescence properties of carbazole and fluorine-based compounds. J Lumin 127:349–354
4. Marder S, Kippelen B, Yen A, Peyghambarian N (1997) Design and synthesis of chromophores and polymers for electro-optic and photorefractive applications. Nature 388:845–851
5. Marder S, Kippelen B, Yen A, Peyghambarian N (1994) Chem Rev 94 (special issue)
6. Lakowicz JR (1999) Principles of fluorescence spectroscopy, 2nd edn. Kluwer, Hingham
7. Li YQ, Bricks JL, Resch-Genger U, Spieles M, Rettig W (2006) Bifunctional charge transfer operated fluorescent probes with acceptor and donor receptors. 2. Bifunctional cation coordination behavior of biphenyl-type sensor molecules incorporating 2,2¢:6¢,2¢-terpyridene acceptors. J Phys Chem A 110:10972–10984
8. Gokel GW, Leevy WM, Weber ME (2004) Crown ethers: sensors for ions and molecular scaffolds for materials and biological models. Chem Rev 104:2723–2750
9. Rettig W (1986) Charge separation in excited states of decoupled systems—TICT compounds and implications regarding the development of new laser dyes and the primary processes of vision and photosynthesis. Angew Chem Angew Chem Int Ed Engl 25:971–988
10. Grabowski ZR, Rotkiewicz K, Rettig W (2003) Structural changes accompanying intramolecular electron transfer: focus on twisted intramolecular charge-transfer states and structures. Chem Rev 103:3899–4031
11. Schopf G, Rettig W, Bendig J (1994) Quenching of TICT fluorescence by electron donors. J Photochem Photobiol A Chem 84:33–37

12. Braun D, Rettig W, Delmond S, Letard J-F, Lapouyade R (1997) Amide derivatives of DMABN: a new class of dual fluorescent compounds. J Phys Chem A 101:6836–6841
13. Malval J-P, Chaimbault C, Fischer B, Morand J-P, Lapouyade R (2001) Optical and electrochemical cations recognition and release from N-azacrown carbazoles. Res Chem Intermed 27:21–34
14. Leray I, Habib-Jiwan J-L, Branger C, Soumillion J-Ph, Valeur B (2000) Ion-responsive fluorescent compounds: VI. Coumarin 153 linked to rigid crowns for improvement of selectivity. J Photochem Photobiol A Chem 135:163–169
15. Habib-Jiwan J-L, Branger C, Soumillion J-Ph, Valeur B (1998) Ion-responsive fluorescent compounds V. Photophysical and complexing properties of coumarin 343 linked to monoaza-15-crown-5. J Photochem Photobiol A Chem 116:127–133
16. Dodiuk H, Cosower EM (1977) Intramolecular donor–acceptor systems. 2.substituent effects on the fluorescence probes: 6-(*N*-Arylamino)-2-naphthalenesulfonamides. J Phys Chem 81:50–54
17. Kossower EM, Dodiuk H, Tanizawa K, Ottolenghi M, Orbach N (1975) Intramolecular donor–acceptor systems. Radiative and nonradiative processes for the excited States of 2-*N*-Arylamino-6-naphthalenesulfonates. J Am Chem Soc 97(8):2167–2178
18. Kanety H, Kosower EM (1982) Multiple fluorescences. 6. The case of 1,8-naphthosultam. J Phys Chem 80:3776–3780
19. Kosower EM, Dodiuk H (1978) Intramolecular donor-acceptor systems. 3. A third type of emitting singlet state for *N*-Alkyl-6-*N*-arylamino-2-naphthalenesulfonates. Solvent modulation of substituent effects on charge-transfer emission. J Am Chem Soc 100 (3):4173–4179
20. Kosower EM (1982) Inramolecular donor–acceptor systems. 9. Photophysics of (Phenylamino)naphthalenesulfonates: a paradigm for excited-state intramolecular charge transfer. Acc Chem Res 15:259–266
21. Kosower EM, Kanety H, Dodiuk H, Striker G, Jovin T, Boni H, Huppert D (1983) Inramolecular donor–acceptor systems. 7. Solvent dielectric relaxation effects on the photophysics of 6-(Phenyamino)-*N,N*-dimethyl-2-naphthalenesulfonamides. J Phys Chem 87:2479–2484
22. Kosower EM, Kanety H (1983) Inramolecular donor–acceptor systems. 10. Multiple fluorescences from 8-(Phenylamino)-1-naphthalenesulfonates. J Am Chem Soc 105:6236–6243
23. Saczewski J, Brzowski Z, Saczewski F, Bednarski PJ, Liebeke M, Gdaniec M (2006) Synthesis and in vitro anti-tumor activity of *N*-{1-[(3-thioxo-5, 6-dihydroimidazo[2,1-c][1,2,4]thiadiazol-7-ylthio)thiocarbonyl]2-imidazolidene}arylsulfonamides. Bioorg Med Chem Lett 16:3663–3667
24. Djakovitch L, Rouge P, Zaidi R (2007) Selective arylation of 2-substituted indoles towards 1,2- and 2,3-functional indoles directed through the catalytic system. Catalysis Communications 8:1561–1566
25. Mann G, Hartwig JF, Driver MS, Fernandez-Rivas C (1998) Palladium-catalyzed C–N (sp^2) bond formation: *N*-arylation of aromatic and unsaturated nitrogen and the reductive elimination chemistry of palladium azolyl methyleneamido complexes. J Am Chem Soc 120:827–828
26. Parker CA (1968) Photoluminescence of solutions. Elsevier, Amsterdam
27. Meech SR, Phillips D (1983) Photophysics of some common fluorescence standards. J Photochem 23:193–217
28. O_Connor DV, Phillips D (1984) Time correlated single photon counting. Academic, London
29. Rettig W, Marschner F (1990) Molecular conformation and biradicaloid charge transfer states in substituted *N*-phenylpyrroles. New J Chem 14:819–824
30. Rettig W, Zander M (1982) On twisted intramolecular charge transfer (TICT) states in *N*-aryl carbazoles. Chem Phys Lett 87:229–234
31. Murali S, Changenet-Barret P, Ley C, Plaza P, Rettig W, Martin MM, Lapuyade R (2005) Photophysical properties of pyrrolobenzenes with different linking and substitution pattern: the transition between charge transfer states with large (MICT) and small (TICT) resonance interaction. Chem Phys Lett 411:192–197
32. Murali S, Rettig W (2005) Meta-positioning effect in sterically hindered *N*-phenyl-pyrroles: a photophysical study. Chem Phys Lett 412:135–140
33. Lippert EZ (1955) Naturforsch 10a:541
34. Mataga N, Kaifu Y, Kazumi M Bull Chem Soc Jpn 1955, 28, 690; 1956, 29, 645
35. Weigel W, Rettig W, Dekhtyrar M, Modrakowski C, Beinhoff M, Schlueter AD (2003) Dual fluorescence of phenyl and biphenyl substituted pyrene derivatives. J Phys Chem A 107:5941–5947